applied sciences

MDPI

Article

Cyclodextrin Polymers as a Promising Drug Carriers for Stabilization of Meropenem Solutions

Linara R. Yakupova, Anna A. Skuredina, Pavel O. Markov, Irina M. Le-Deygen and Elena V. Kudryashova *

Chemistry Department, Lomonosov Moscow State University, 119991 Moscow, Russia
* Correspondence: helena_koudriachova@hotmail.com

Abstract: Here we report the development of new drug carriers for meropenem based on the hydroxypropyl-β-cyclodextrin (HPCD) polymers with variable linkers, namely, 1,6-hexamethylened-iisocyanate (HMD), citric acid (CA), succinic anhydride (SA). The structures of obtained polyesters and polyurethanes nanoparticles (120–200 nm) were investigated by NMR and FTIR-spectroscopy. The PXRD pattern demonstrated that HPCD polymers form complexes with meropenem (MP), and the majority of MP molecules are encapsulated into a complex. MP's imprinting in the HPCD-HMD polymer matrix lead to an encapsulation efficiency of up to 82%. HPCD-HMD and HPCD-SA polymers increase MP's stability during the storage of its aqueous solution (in 1.4 and 1.2 times, respectively). In contrast, HPCD-CA polymer negatively affects MP's stability. In prospect, the HPCD-HMD polymer may be promising for the development of a highly efficient drug delivery system for MP.

Keywords: cyclodextrin polymers; meropenem; drug delivery

Citation: Yakupova, L.R.; Skuredina, A.A.; Markov, P.O.; Le-Deygen, I.M.; Kudryashova, E.V. Cyclodextrin Polymers as a Promising Drug Carriers for Stabilization of Meropenem Solutions. *Appl. Sci.* **2023**, *13*, 3608. https://doi.org/10.3390/app13063608

Academic Editors: Sergey A. Milenin, Fedor Valerevich Drozdov and Anton A. Anisimov

Received: 20 February 2023
Revised: 7 March 2023
Accepted: 10 March 2023
Published: 11 March 2023

1. Introduction

Today, multidrug-resistant bacteria provide a severe threat for people all over the world, and very few antibiotics, mostly from the reserve group (according to the WHO AWaRe classification), are available for treatment of this kind of infection [1].

Meropenem (MP) is one the key antibacterial drugs active against several resistant bacteria [2,3]. MP inhibits cell wall synthesis and usually provides bactericidal effects with a wide spectrum of action including Gram-negative along with *Enterobacteriaceae* family and Gram-positive bacteria [4]. Despite high antibacterial activity, the application of MP in therapy is still limited due to its low solubility in aqueous media and rapid degradation upon storage [5]. In order to overcome these drawbacks, one should apply drug delivery systems (DDS) with improved biopharmaceutical properties and high biocompatibility. Moreover, there are several more requirements for DDS, e.g., high encapsulation efficacy, long-term stability upon storage, prolonged release, etc. One of the most promising DDS for MP are β-cyclodextrins (CD), cyclic oligosaccharides consisting of seven glucopyranose units linked by α-(1,4)-bonds. CDs are produced from starch using enzymatic conversion by cyclodextrin glycosyltransferases and α-amylases, thus CD are biocompatible and biodegradable [6,7].

The glucopyranose units in CD create a torus-like structure with a hydrophilic outer surface, which defines CD's high solubility in water and hydrophobic cavity, suitable for "guest-host" complex formation with hydrophobic drugs [8]. The formation of a complex with CD improves solubility, stability, and bioavailability of the drugs, furthermore, CDs are approved by the FDA as DDS [9]. Several researchers have demonstrated that CD strengthens drug absorption through the biological barriers, including the blood-brain barrier, because of changing drug-transport properties through lipophilic barriers and affecting membrane fluidity to reduce the barrier function [6,10–12].

Besides initial CDs, many up to date CD derivatives have been synthesized by reactions of esterifications, etherifications, or aminations [10]. The modified CD provides enhanced solubility and stability against oxidation and light, also different substituents regulate the chemical activity of CD [6,13].

However, when it comes to the fine tailoring of DDS and managing the biopharmaceutical properties of final drug formulation, one desires additional DDS's properties, for instance, prolonged drug release and the increased bioavailability. From this perspective, the new era of CD-based DDS is coming with CD polymers constructed from different CDs united in one molecular structure by means of small molecules—linkers. Upon shifting from monomeric CDs to polymeric systems, one discovers several new parameters, such as the degree of polymerization, the nature of the linker, the density of crosslinks, etc., which will potentially allow fine-tuning the DDS and obtain its desirable properties. Moreover, significant dosage reduction and simplification of drug regimens can be achieved using CD polymers [10]. Thus, the main benefits of CD polymers as DDS make them potentially applicable for MP delivery to overcome the severe infections that are caused by multidrug resistant bacteria.

Here, we aimed to design DDS for MP based on the polymers of 2-hydroxypropyl-β-CD (HPCD) and investigate the main patterns of interaction between the drug and carrier by the various spectroscopic methods.

2. Materials and Methods

2.1. Materials

2-hydroxypropyl-β-cyclodextrin, NaH_2PO_4, meropenem, 1,6-hexamethylenediisocyanate (HMD), citric acid (CA), succinic anhydride (SA), dimethyl sulfoxide (DMSO), are all from Sigma-Aldrich (St. Louis, MO, USA). HCl was purchased from Reakhim (Moscow, Russia). Tablets for sodium-phosphate buffer solution preparation (pH 7.4) were obtained from Pan-Eco (Moscow, Russia).

2.2. Methods

2.2.1. Synthesis of HPCD Polymers Linked by CA and SA

A total of 300 mg of 2-hydroxypropyl-β-cyclodextrin (HPCD) was dissolved in distilled water (C_{HPCD} = 60 mg/mL). Then, 75 mg of the catalyst (NaH_2PO_4) was added to the solution, which was heated to 140 °C. After that, the required quantity of the linker's aqueous solution (3 M of citric acid (CA) or succinic acid (SA)) was added dropwise. The HPCD:linker molar ratios were 1:15 for both linkers. The final volumes of the reaction mixtures were 6 mL. The solutions were stirred for 1.5 h with heating at 140 °C. The purification of HPCD polymers from unreacted reagents and catalyst was carried out by dialysis (cut-off molecular weight 12 kDa membrane, Serva, Heidelberg, Germany) for 4 h at room temperature with intensive shaking and the regular external solution replacement (1.0–1.2 L of distilled water). The samples were poured into sterile Petri dishes and dried for 24 h at 25 °C on a thermos-controlled shaker-incubator ES-20 (Biosan, Riga, Latvia).

2.2.2. Synthesis of HPCD Polymer and HPCD Polymer with Encapsulated MP Linked by HMD

The HPCD polymer synthesis using 1,6-hexamethylene diisocyanate was conducted according to [14]. Briefly, into 3 mL of the warm HPCD aqueous solution (C_{HPCD} = 100 mg/mL), 2.964 mL DMSO was added dropwise. After 5 min, 36 μL HMD was added dropwise to the reaction mixture, which then was stirred for 1 h. The HPCD:linker molar ratio was 1:5.

For HPCD polymer with imprinted MP (HPCD-HMD-MP_{im}), the HPCD-MP complex was used as a monomer. The complex of HPCD—meropenem (MP) in a molar ratio of 1:1 (C = 0.015 M) was obtained by the mixture of aqueous solutions of individual components. The solution was stored at 37 °C for 30 min. Then, the DMSO and HMD were added dropwise in accordance with HPCD-HMD synthesis.

The purification of HPCD-HMD and HPCD-HMD-MP_{im} was conducted by dialysis as was described for HPCD-CA and HPCD-SA.

The concentration of CD-torus in HPCD polymers was detected by FTIR spectroscopy. We used the calibration curve that was obtained for the 1032 cm^{-1} band that corresponds to the C-O-C bond vibration of HPCD.

The MP's encapsulation efficiency was calculated in accordance with MP's concentration in HPCD-HMD-MP_{im} (revealed by FTIR spectrum), which was compared with the initial MP's concentration used in the synthesis.

2.2.3. MP Stability Studies

Determination of MP stability in an aqueous solution was carried out by analyzing the UV and FTIR spectra of MP. First, aqueous solutions of MP and its complexes with HPCD polymers were prepared (MP:HPCD-tours in polymers molar ratio was 1:1). For all samples, the MP's concentration was 0.01 M. The UV-spectra and FTIR spectra were recorded at regular intervals for two weeks. The analysis of the spectra was carried out using the Opus 7.0 software (Bruker, Ettlingen, Germany).

2.2.4. MP Release Studies

A total of 1.5 mL of MP-HPCD polymer complex aqueous solution (C_{MP} = 0.3 mM) was transferred to a dialysis bag (cut-off molecular weight 12 kDa membrane, Serva, Heidelberg, Germany), which was put into 1.5 mL H_2O. The samples were stirred at 37 °C on a thermo controlled shaker and the external solution was analyzed every 10–15 min by UV spectroscopy.

2.2.5. Optical Microscopy

The microphotographs were obtained using the optical system of NTEGRA II AFM (NT-MDT, Zelenograd, Moscow, Russia).

2.2.6. UV-Spectroscopy

The UV-spectra were registered by Ultrospec 2100 pro device (Amersham Biosciences, Amersharm, UK). An absorption spectrum of MP was recorded in a wavelength range from 200 to 450 nm in a quartz cell with a volume of 1 mL (Hellma Analytics, Jena, Germany). The absorption maximum for freshly prepared MP was at λ_{max} = 297 nm, and for hydrolyzed MP, two low-intensity peaks were observed at wavelengths of 266 and 334 nm. The concentrations of the measured samples were approximately 1×10^{-4} M.

2.2.7. NMR-Spectroscopy

^{1}H-NMR spectra were recorded on a Bruker Avance 400 spectrometer (Reinshtetten, Germany) at 400 MHz in D_2O referenced to HDO (4.75 ppm). For each spectrum 10–15 mg of sample was used.

2.2.8. FTIR-Spectroscopy

The FTIR-spectra were obtained by using a Tensor 27 spectrometer (Bruker, Ettlingen, Germany) equipped with an MCT detector cooled with liquid-nitrogen, as well as a thermostat (Huber, Offenburg, Germany), ZnSe single-reflection crystal, and a cell with attenuated total reflection (Bruker, Ettlingen, Germany). A total of 40 μL of the samples were placed in a cell and their IR-spectra were detected three times (70 scans each time) in the range of 2200–900 cm^{-1} with a resolution of 1 cm^{-1} at room temperature (22 °C). The system was purged with dry air using an air compressor (Jun-Air, Munich, Germany). The background spectrum (water or buffer solution) was registered in the same way. The analysis of the spectra was carried out using the Opus 7.0 program (Bruker, Ettlingen, Germany).

2.2.9. Nanoparticle Tracking Analysis (NTA)

NTA was carried out using the Nanosight LM10-HS device (Nanosight Ltd., Malvern, UK). The HPCD polymers were dissolved in Milli-Q purified water in the amount of 1 mg/mL, and then were diluted to obtain the solutions with the suitable concentration of the particles (~10^8 particles/mL). The measurements were performed five times for each sample. The values are provided with standard deviations.

2.2.10. Molecular Weight of HPCD Polymers

HPCD polymers' Mr was determined by the following formula:

$$\mathrm{Mr} = \frac{[CD] \times NA}{n} \times M_{rm}$$

where the number of the particles n (particles/mL) was obtained by NTA [15]. Other parameters include Avogadro constant N_A, the concentration of CD torus [CD] (mole/mL) in accordance with dilution. Mr_m is the repeating unit's molecular weight (CD and linker).

2.2.11. Dynamic Light Scattering (DLS)

The determination of the HPCD polymers' ζ-potentials were performed using the DLS method (Zetasizer Nano S «Malvern» with 4 mW He–Ne-laser, 633 nm; Malvern, UK) at 25 °C. The analysis was performed three times for each sample using the correlation of the Correlator system K7032-09 «Malvern» (Malvern, UK) and «Zetasizer Software» software v.6.32. The values are provided with standard deviations.

2.2.12. Powder X-ray Diffraction (PXRD) Analysis

For PXRD analysis, HPCD polymer—MP complexes were obtained by grinding the dry components in a mortar of (9 mg of MP powder with 9 mg of dried HPCD polymer) for 5 min. The PXRD patterns were registered by a Rigaku SmartLab (Tokio, Japan) equipped with a copper X-ray anode tube. The settings for X-ray generation were 60 kV and 1.5 kW. The scanning range was 1.5–80.0° in increments of 5° per second.

3. Results and Discussion

In this work, we aimed to design DDS for MP based on the polymers of HPCD (Figure 1). As cross-linking agents, we have considered three different molecules, namely, citric acid (CA), succinic anhydride (SA), and 1,6 hexamethylene diisocyanate (HMD). Since the size, charge, and structure of HPCD polymers might affect the binding of MP and consequently, its stability, we obtained drug carriers with various functional characteristics. The structure differences of synthesized HPCD polymers (HPCD-CA, HPCD-SA and HPCD-HMD correspondingly) as well as their physical-chemical properties might be crucial for interaction with MP.

The morphology of solid HPCD polymers differ dramatically (Figure S1): HPCD-CA is a highly viscous colorless gel-like substance, whereas HPCD-SA forms transparent colorless glass-like crystals. In the case of the HMD linker, the polymers appear as white powder. After the preparation of the samples' solutions, we noted that HPCD-HMD is less soluble than HPCD-CA and HPCD-SA. Thus, the nature of the cross-linking agent dramatically influences even the physical state of the DDS.

In order to reveal how MP might affect the formation of the HPCD polymer matrix, we also synthesized molecularly imprinted DDS, where the HPCD-MP guest-host complex was used as a monomer—HPCD-HMD-MP_{im} (Figure 1). Thus, MP might be molecularly imprinted into the final polymer matrix. Such systems are of great interest because of sustained drug release and prolonged antibacterial activity [16,17]. For CA and SA linkers such an approach is not possible due to the high temperature via synthesis that might cause MP's degradation. As such, the main difference between two types of DDS here is that for HPCD-CA, HPCD-SA, and HPCD-HMD, the first step was cross-linking followed by drug encapsulation, while for HPCD-HMD-MP_{im} the order of stages was exactly the opposite.

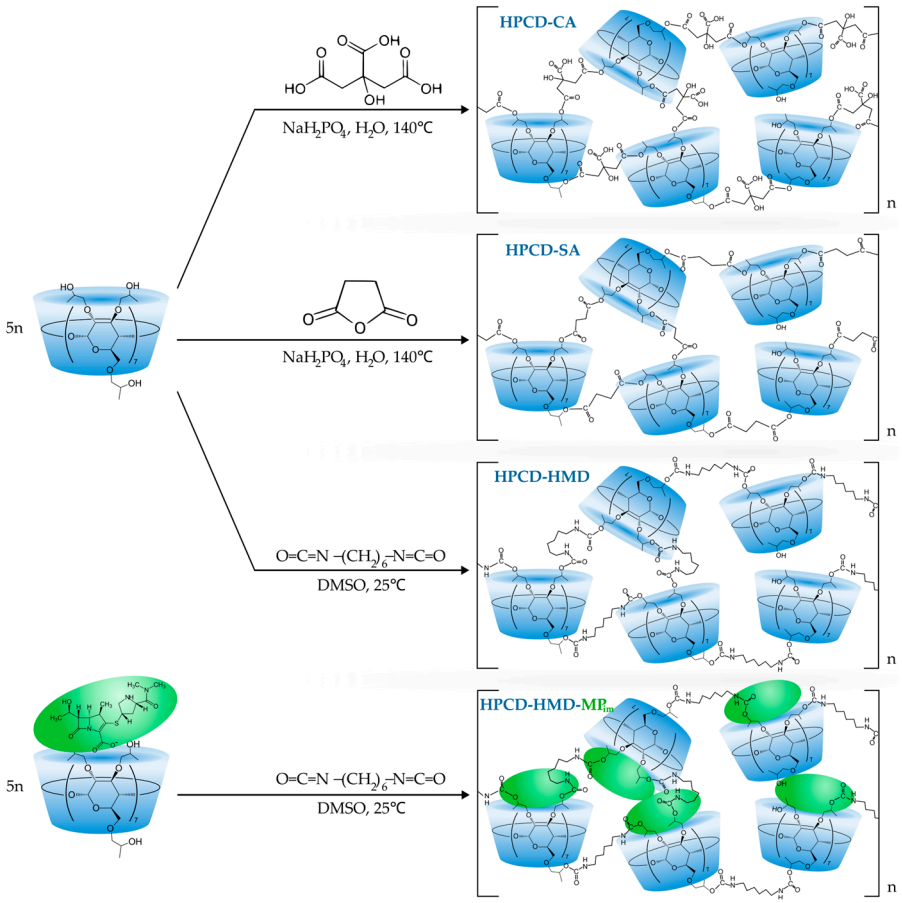

Figure 1. The scheme of HPCD-Citric acid, HPCD-Succinic acid, HPCD-HMD, and HPCD-HMD-MP_{im} polymer synthesis.

3.1. DLS and NTA Analysis

It is well-known, that HPCD polymerization yield large molecules [18] that are able to form nanoparticles. As such, in order to evaluate the role of cross-linking agents we compared hydrodynamic diameters and ζ-potentials for all types of synthetized polymers via nanoparticle tracking analysis (NTA) and dynamic light scattering (DLS) [19].

The obtained data are summarized in Table 1. According to NTA data, the HPCD polymers form homogeneous nanoparticles with an average diameter of 150 nm. The DLS provided higher values (250–300 nm) that might be caused by the presence of hydrophilic particle's shell.

Table 1. The size and ζ-potential of HPCD polymers, H_2O, 25 °C.

	Method	HPCD	HPCD-CA	HPCD-SA	HPCD-HMD	HPCD-HMD-MP_{im}
Hydrodynamic diameter, nm	NTA	≈0.15 [1]	120.1 ± 3.2	199.2 ± 18.2	142.5 ± 13.5	178.8 ± 10.2
	DLS	≈0.15 [1]	245 ± 15	283 ± 21	220 ± 17	289 ± 22
ζ-potential, mV	DLS	0.5 ± 0.3	– [2]	5.6 ± 2.1	14.7 ± 0.4	−2.9 ± 0.3

[1]—the size of HPCD is assumed as the size of β-CD [6]; [2]—ζ-potential of HPCD-CA isn't determined, since a chemical reaction may occur under the experimental conditions (decarboxylation).

The average size of HPCD-CA polymers is smaller than HPCD-SA, apparently due to the three functional groups in CA that are available for binding which might cause the formation of a denser polymer structure.

HPCD-HMD demonstrates the hydrodynamic diameter of approximately 150 nm, while MP's imprinting into HPCD-HMD polymer leads to the slight increase of particle size.

We suppose this effect might be caused by the complexation of MP with HPCD at the first synthesis stage, which increases the spatial distance between CD-torus for linker binding.

The ζ-potential value usually represents valuable data for colloidal particles and, in the case of HPCD-CA, the determination of accurate values was challenging. We suppose a chemical reaction (decarboxylation of a free carboxyl group) may occur under the experimental conditions. Nevertheless, we expect negative surface charge. For HPCD-SA (synthesized with bifunctional linker), the ζ-potential is close to neutral. Interestingly, HPCD-HMD demonstrates strong positive ζ-potential. This finding will be discussed further.

In the case of HPCD-HMD-MP_{im}, the ζ-potential is significantly lower. MP is predominantly zwitterionic in aqueous solution [20], and its ζ-potential is −3.72 mV [21]. MP's imprinting into HPCD polymer matrix lead to the decrease of particles' ζ-potential that might be due to interactions between MP and the HPCD-HMD polymer network. We have recently obtained similar results for resembling imprinted systems based on sulfobutyl ether β-cyclodextrin, HMD, and moxifloxacin [22]. The imprinting of moxifloxacin in cyclodextrin's matrix causes the neutralization of particles' ζ-potential. We would like to stress that moxifloxacin was uniformly distributed over the entire volume of the particle. Thus, we assume that cyclodextrin polymers with imprinted MP or moxifloxacin might have similar properties.

Thus, the comparison of the data from DLS and NTA reveals significant differences between both two types of DDS (imprinted and not imprinted) and between polymers that were obtained with different cross-linking agents. The average Mr value is 150 kDa. In order to discover the physico-chemical reasons of this phenomenon we have studied the structure of obtained systems in detail via spectroscopic methods.

3.2. The Structure of HPCD-Polymers

In order to prove the chemical structure of the obtained polymers, we have used ATR-FTIR and ^{1}H NMR spectroscopy.

In the FTIR spectra of HPCD, we observed the most intense absorption bands in the 1100–1000 cm^{-1} region corresponding to C–O–C glycoside bonds (Figure 2A) [23]. The formation of HPCD-CA leads to the appearance of bands 1725 cm^{-1} and 1226 cm^{-1} regarding to C=O in carboxylic and ester groups and C-O-C in ester groups, respectively [24]. Interestingly, the CA spectrum contains the band at 1720 cm^{-1} (C=O st). The shift of the band to the higher wave numbers in HPCD-CA spectrum indicates the formation of ester bonds that was demonstrated, for instance, via chemical linkage between starch and CA in [25].

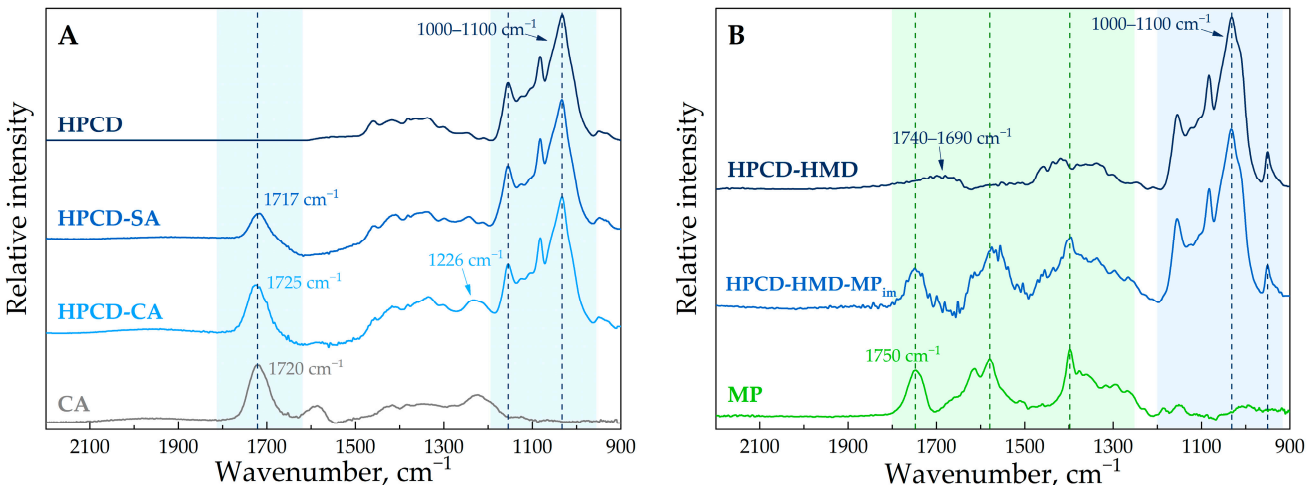

Figure 2. Normalized FTIR spectra of (**A**) HPCD, HPCD-Succinic acid polymer, HPCD-Citric acid polymer, and citric acid; (**B**) HPCD-HMD, HPCD-HMD-MP_{im}, and MP in the range of 2200–900 cm^{-1}, H_2O, 22 °C.

For HPCD-SA, we observed a similar pattern as for HPCD-CA (Figure 2A). The appearance of an intense band at 1717 cm^{-1} corresponding to the C=O group in the polymer network. Thus, the formation of two ester polymers was confirmed.

In the case of the HMD cross-linker, we expected the formation of a polyurethane bond with a typical band around 1740–1700 cm^{-1} of the C=O group in the FTIR spectra [26,27]. Indeed, for HPCD-HMD, we observed a wide band in the region of 1740–1690 cm^{-1} (Figure 2B). Moreover, the 951 cm^{-1} band appears, which corresponds to the C-N bond in primary amines [28]. This functional group might appear via the hydrolysis of unreacted isocyanate groups in aqueous media that was demonstrated earlier for cross-linked hydroxyethyl starch nanocapsules [27]. In addition, the positive ζ-potential of the HPCD-HMD confirms the presence of $–NH_2$ groups on the surface of the particles (Table 1).

In the FTIR spectra of HPCD-HMD-MP_{im} (Figure 2B), we observed the bands that are characteristic for both MP and HPCD-HMD polymers. MP probably does not influence the synthesis process of polymeric networks. We suppose MP is physically entrapped into the polymer matrix on molecular level and is not chemically modified. Thus, MP retains its antibacterial activity.

For a deeper study on how the imprinting affects MP's state in HPCD-HMD-MP_{im} (MP_{im}), the FTIR spectrum of HPCD-HMD was subtracted from the FTIR spectrum of HPCD-HMD-MP_{im} (Figure S2). We found that the MP_{im}'s FTIR spectra is similar to the FTIR spectra of free MP. The determined MP's encapsulation efficiency is 82 ± 4% (compared to the initial C_{MP} used in the synthesis), which means that the major part of drug molecule was imprinted into the polymer matrix. As such, the carrier's capacity is 0.13 mg per 1 mg of the sample. Previously, similar inclusion efficacy was obtained for imprinted moxifloxacin; more than 80% is immersed in the polymer structure [22].

Surprisingly, we observed two pronounced changes in the FTIR spectra of MP_{im}; the structural changes in the peak in the 1700–1500 cm^{-1} region and the decrease of the 1750 cm^{-1} peak's intensity. We will describe it in more detail as it reveals the most interesting changes in the MP's microenvironment upon complex formation.

The effect of 1750 cm^{-1} band intensity decreasing might indicate the participation of MP's carboxylic group in hydrogen bonding via complex formation with HPCD polymer matrix, as it was demonstrated previously for MP-CD complex in [2]. If this band corresponds to the carboxylic group, this spectral region has to be pH-sensitive. In the independent experiment, we compared spectral patterns for MP solutions with various pH values (Figure 3).

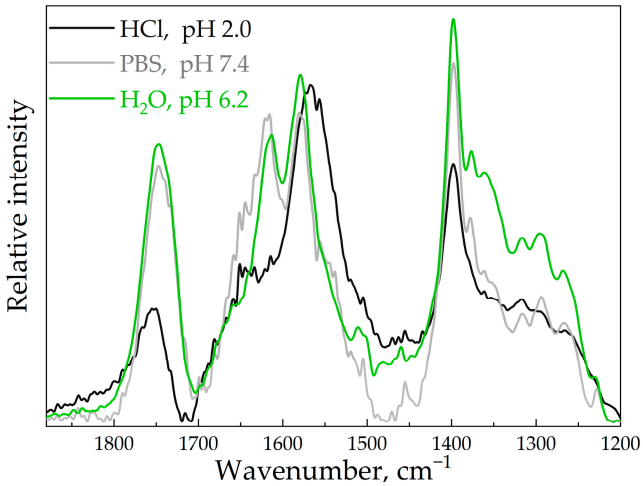

Figure 3. The normalized FTIR spectra of MP in acidic (pH 2.0; HCl), neutral (distilled water), and slightly alkaline (pH 7.4; 0.01 M sodium-phosphate buffer solution) media, 22 °C.

According to the spectral data, this region is definitely pH-sensitive. The 1615 and 1579 cm^{-1} bands are assigned to vibrations of the C=O bond and CH_3-group in dimethyl

carbamoyl fragments in MP's structure, respectively [29]. At low pH values, we observed the pronounced decrease of 1615 cm^{-1} band intensity. Such structural changes in MP's FTIR spectra might be caused by the MP's hydrolysis. Thus, during encapsulation, MP degrades to some extent, which may be due to prolonged contact with water via synthesis. Nevertheless, its moiety is entrapped in the polymer matrix, which will prevent it from undergoing further hydrolysis, so we assume MP imprinting in the HPCD polymer matrix might increase its stability.

^{1}H NMR spectroscopy confirms the polymers formation (Figures 4 and S3). Briefly, the multiplet at δ 3.40–4.11 ppm refers to H2–H5 of the D-glucopyranose units, signals at δ 5.01–5.31 ppm to H1 of the D-glucopyranose units and doublet at δ = 1.13 ppm, J = 6.2 Hz to the protons of the hydroxypropyl substituent, respectively [14]. In ^{1}H NMR spectra of all HPCD polymers, we observed the signals that correlate to both the monomer and the linker. In the case of HPCD-HMD-MP$_{im}$, the peaks that were assigned to MP are also present in the spectrum [30].

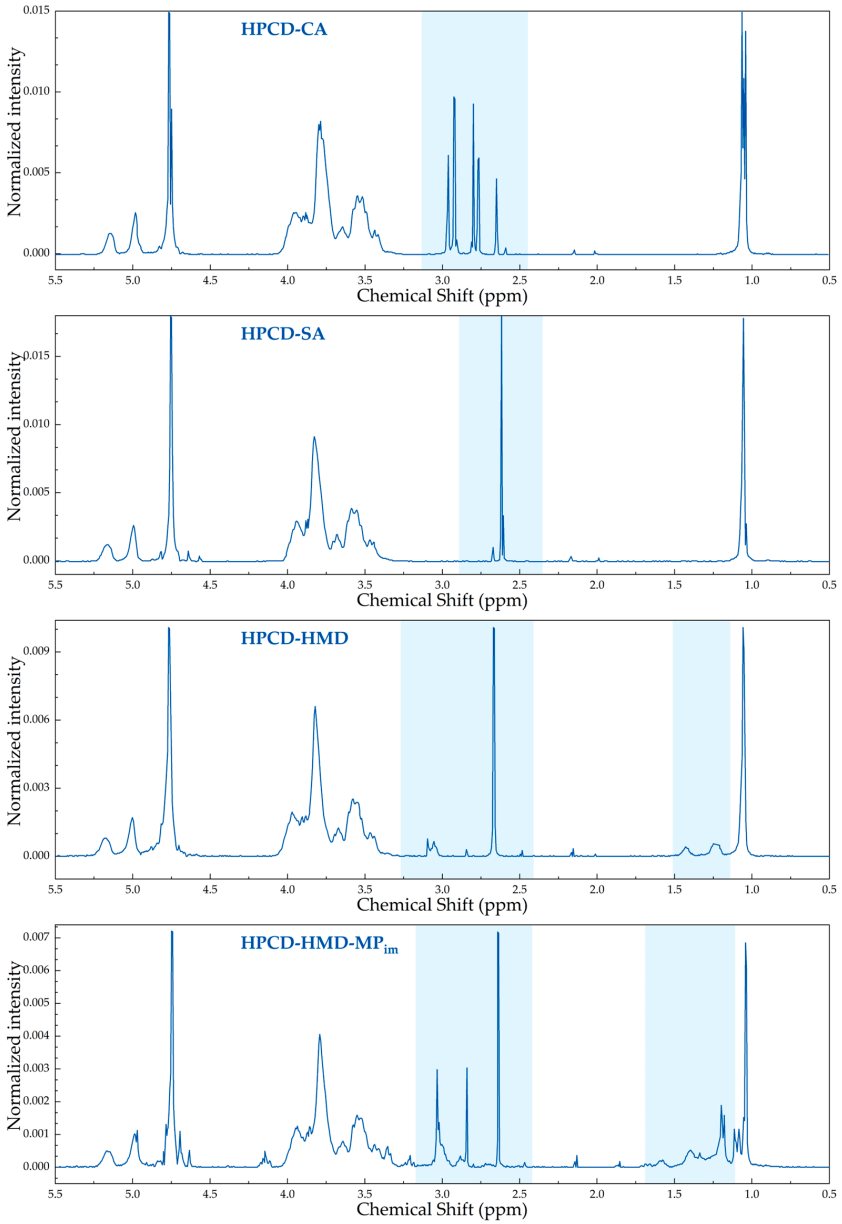

Figure 4. ^{1}H NMR of HPCD, HPCD-CA polymer, HPCD-SA acid polymer, HPCD-HMD, and HPCD-HMD-MP$_{im}$, D_2O, 400 MHz. The blue shading indicates the peaks corresponded to the linkers.

In the case of the polymers that were synthesized without MP (Figure 1), we obtained polymer-drug complexes by kneading technique, avoiding preliminary contact with water. We studied these systems by powder X-ray diffraction (PXRD) to confirm the complex formation and uncover how HPCD polymers affect the MP's properties via incorporation into a polymeric network in a solid state.

The PXRD pattern of MP (Figure 5) corresponds to a crystalline drug (CSD# 1287245) [31,32]. The PXRD patterns for CDs are commonly reported [33] with the predominance of amorphous phase. The formation of the complexes between drug molecules and CDs as well as their polymers often changes the drug's degree of crystallinity [18,34]. Indeed, in our case, MP-HPCD polymer complex formation leads to pronounced changes in PXRD pattern; the degree of crystallinity measured at the integral intensities of the «halo» and crystalline peaks is around 20%.

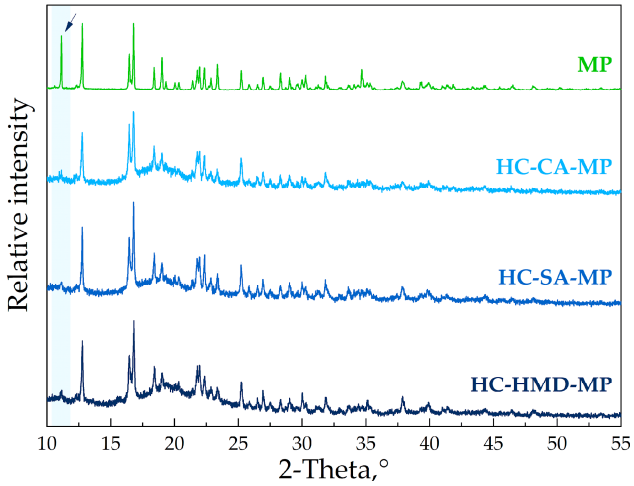

Figure 5. Experimental PXRD patterns for MP, HPCD-CA-MP, HPCD-SA-MP, and HPCD-HMD-MP. No more signals were detected from 55° to 80°.

All HPCD polymers change MP's PXRD pattern to the similar extent. Thus, in the solid state the main part of MP is complexed with HPCD polymers.

Analysis of the PXRD curves shows that complex formation with polymeric carriers leads to the disappearance of one of MP's reflections at small angles. This interesting reproducible effect indicates a change in the orientation of the meropenem molecules, apparently due to the binding with polymers. It is known that it is the packing change that leads to the disappearance of some reflections from the PXRD pattern [35]. Thus, the inclusion of meropenem in tori of HPCD polymers is confirmed by PXRD data.

3.3. The Influence of HPCD Polymers on MP's Stability in Aqueous Media

Due to the presence of a β-lactam ring in the drug's structure (Figure 1), MP degrades in aqueous solution. The chemical changes in MP's pharmacophore causes the loss of its antibacterial activity [20,36,37]. MP's instability in water is even visually noticeable, since the solution changes its color from transparent to brown during storage.

MP's state can be successfully monitored using UV-spectroscopy. Freshly prepared MP solution (fMP) demonstrates the peak at 297 nm (Figure 6), whereas after 2 months of storage (sMP), we observed two low-intensity peaks at 269 and 333 nm. Consequently, MP's degradation rate can be tracked by the intensity and the position of the initial peak.

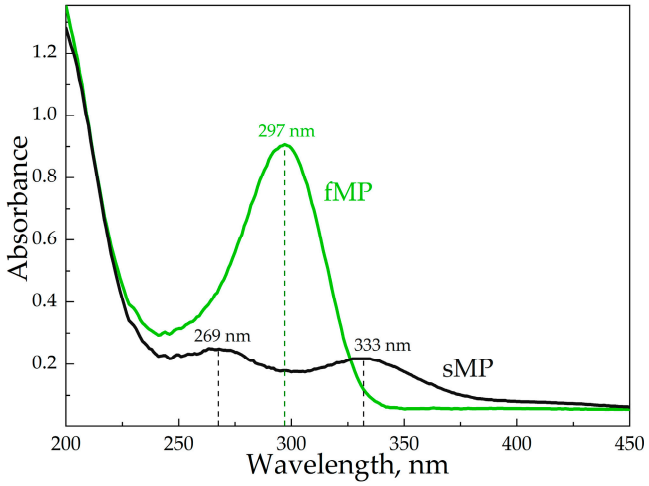

Figure 6. UV-spectra of freshly prepared MP solution (fMP) and the solution, stored for 2 months (sMP), C_{MP} = 0.1 mM.

The UV's peak of fMP decreases after 5 h of storage at room temperature and the decline occurs by 35% in 9 days (Figure 7). MP-HPCD polymer complexes were also studied to uncover how particles affect MP's stability. In the case of HPCD-CA-MP, we determined a significant acceleration of the drug's degradation; MP's peak intensity decreased dramatically after a few hours (3 times in 5 h and 4 times in 3 days).

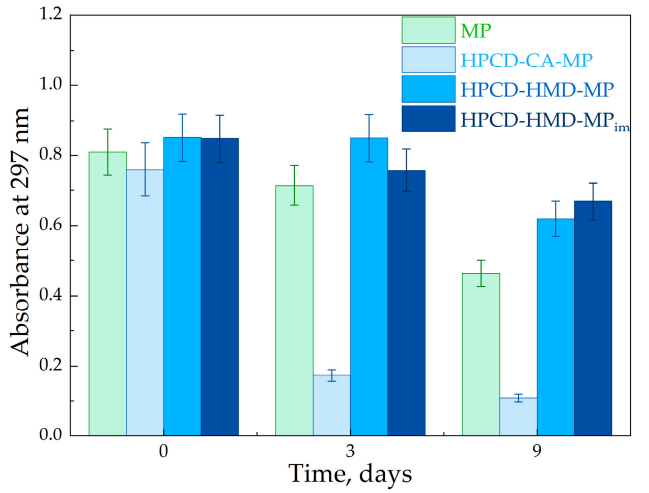

Figure 7. The diagram of MP's spectrum intensity at 297 nm for MP, HPCD-CA-MP, HPCD-HMD-MP, and HPCD-HMD-MP_{im}, T = 22 °C.

In contrast, for HPCD-SA-MP and HPCD-HMD-MP a positive effect on the drug's stability was observed during the entire time interval. MP's stability increases for 1.2 and 1.4 times in 9 days for HPCD-SA-MP and HPCD-HMD-MP, respectively, compared to the free MP. Unlike HPCD-CA, these polymers have positive and neutral charges. Consequently, the negative charge of the carrier accelerates MP's degradation, possibly due to environmental acidification.

Unexpectedly, HPCD-HMD-MP_{im} with imprinted drug molecules demonstrated a similar effect on MP's stability that was found for HPCD-SA-MP and HPCD-HMD-MP. The probable reason is the hydrophilic structure of the MP due to which it is involved mainly in electrostatic interactions. Since HMD forms hydrophobic pores in the polymer, electrostatic interplay is the same for imprinted and encapsulated drug-carriers.

Throughout the experiment of MP's stability, during the storage the samples were also studied by FTIR spectroscopy. As discussed above, the 1613 cm^{-1} peak might be

sensitive to MP's degradation. To prove this statement, we obtained FTIR spectra of MP during 9 days (Figure 8). Indeed, the band's intensity decreased dramatically during MP's storage. Thus, the analysis of this effect for MP-HPCD polymers is informative for uncovering MP's degradation extent. The FTIR data proved all trends that were obtained by UV-spectroscopy.

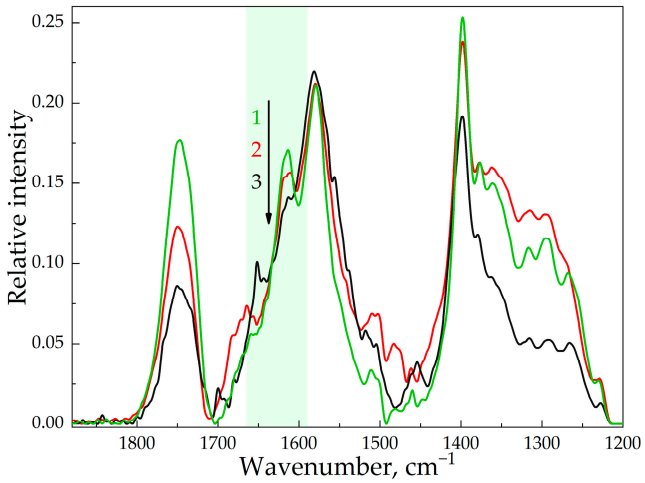

Figure 8. The normalized FTIR spectra of "fresh" MP solution (1) and MP solution stored for 1 day (2) and 6 days (3), C_{MP} = 0.01 M, 22 °C.

3.4. The Influence of HPCD Polymers on MP's Release

Free MP is released from the model dialysis bag by about 80% in 60 min (Figure 9). All polymers slow down MP's release rate and this effect is more significant for polymers that were synthesized with HMD; less than 70% of MP is released in 2 h. The holding forces are probably electrostatic, since MP is a hydrophilic molecule. As a result, MP is not held in the pores of the polymer with the most hydrophobic linkers (HMD), but interacts with charged primary amines, which occur via the hydrolysis of unreacted isocyanate groups in aqueous solution. The positive charge of the polymer's surface also contributes to the retention of MP on nanoparticles (Table 1).

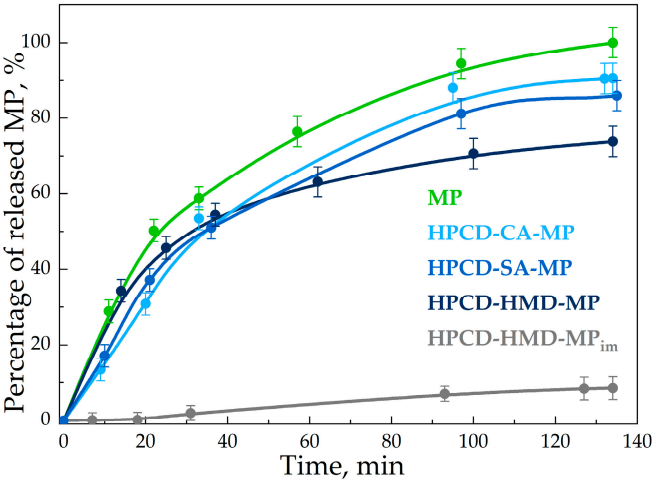

Figure 9. The release kinetics of MP, HPCD-CA-MP, HPCD-SA-MP, HPCD-HMD-MP, and HPCD-HMD-MP_{im}, C_{MP} = 0.3 mM, 37 °C.

Remarkably, HPCD-HMD-MP_{im} greatly reduces MP's release rate; less than 10% of MP is released on the first day and less than 30% on the third day. Such a drug carrier with imprinted MP promotes the creation of a prolonged release system. Indeed, for imprinted moxifloxacin in cyclodextrin matrix [22], we observed a similar release rate of less than

30% of the drug in 10 days. Importantly, the fixation of MP inside the polymer's matrix contributes to the preservation of MP's structure and prolonged release of the active drug, makes a prolonged therapeutic effect possible.

4. Conclusions

In this work we synthesized polymers based on HPCD using different linkers, HMD, citric acid, and succinic anhydride, in order to use them as drug carriers to stabilize MP's aqueous solution during storage. The cross-linking of HPCD led to nanoparticle formation of polyesters and polyurethanes, respectively, that were studied by NTA, DLS, NMR, and FTIR-spectroscopy. PXRD experiments demonstrated that HPCD polymers form complexes with the drug MP and the major part of it is encapsulated in the polymer matrix. Moreover, via template synthesis, we obtained the polymer with imprinted MP. In this case, the degree of MP imprinting into the polymer matrix is 82%.

Using UV- and FTIR-spectroscopy, we uncovered that HPCD-CA polymer significantly decreases MP's stability, which becomes noticeable after a few hours. The probable cause of this effect is environmental acidification. In contrast HPCD-HMD and HPCD-SA polymers positively affect MP stability, which increases for 1.2- and 1.4-times in 9 days for HPCD-SA-MP and HPCD-HMD-MP, respectively, compared to the free MP. HPCD-HMD-MP_{im} showed a similar effect on MP's stability, which can be explained by the electrostatic nature of the interactions of MP with the drug carrier, which are the same for imprinted and encapsulated drug-carriers.

Therefore, we conclude that HMD and SA cross-linking agents are promising to develop highly effective MP's formulation.

Supplementary Materials: The following supporting information can be downloaded at: https://www.mdpi.com/article/10.3390/app13063608/s1, Figure S1: Micrographs of A. HPCD-CA; B. HPCD-SA; C. HPCD-HMD and photographs of D. HPCD-CA; E. HPCD-SA; F. HPCD-HMD; Figure S2: The normalized FTIR spectra of MP and MP_{im} (the FTIR spectrum of HPCD-HMD was subtracted from FTIR spectrum of HPCD-HMD-MP_{im}), 22 °C; Figure S3. ^{1}H NMR of HPCD, CA, SA, D_2O, 400 MHz.

Author Contributions: Conceptualization: A.A.S. and E.V.K.; Experimental work, data analysis, and interpretation: L.R.Y., P.O.M., I.M.L.-D. and A.A.S.; Writing—original draft preparation: L.R.Y. and A.A.S.; Writing—Review and editing: A.A.S., L.R.Y., I.M.L.-D. and E.V.K.; Supervision: A.A.S. and E.V.K. All authors have read and agreed to the published version of the manuscript.

Funding: This work was supported by the Russian Science Foundation grant number 22-24-00604.

Institutional Review Board Statement: Not applicable.

Informed Consent Statement: Not applicable.

Data Availability Statement: Not applicable.

Acknowledgments: The work was performed using equipment (NTEGRA II AFM and FTIR spectrometer Bruker Tensor 27) of the program for the development of Moscow State University, and equipment purchased by the Developmental Program of Lomonosov Moscow State University (PNR 5.13). The work was supported by the Scholarship of the President of the Russia for young scientists and postgraduates (for A.A.S.).

Conflicts of Interest: The authors declare no conflict of interest.

References

1. Sulis, G.; Sayood, S.; Katukoori, S.; Bollam, N. Exposure to WHO AWaRe antibiotics and isolation of multi-drug resistant bacteria: A systematic review and meta-analysis. *Clin. Microbiol. Infect.* **2022**, *28*, 1193–1202. [CrossRef]
2. Paczkowska, M.; Mizera, M.; Szymanowska-Powałowska, D. β-Cyclodextrin complexation as an effective drug delivery system for meropenem. *Eur. J. Pharm. Biopharm.* **2016**, *99*, 24–34. [CrossRef]
3. Raza, A.; Miles, J.; Sime, F.; Ross, B.; Roberts, J. PLGA encapsulated γ-cyclodextrin-meropenem inclusion complex formulation for oral delivery. *Int. J. Pharm.* **2021**, *597*, 120280. [CrossRef]
4. Edwards, J.R. Meropenem: A microbiological overview. *J. Antimicrob. Chemother.* **1995**, *36*, 1–17. [CrossRef]

5. Mendez, A.; Dalomo, J.; Steppe, M. Stability and degradation kinetics of meropenem in powder for injection and reconstituted sample. *J. Pharm. Biomed. Anal.* **2006**, *41*, 1363–1366. [CrossRef]
6. Martin Del Valle, E.M. Cyclodextrins and their uses: A review. *Process Biochem.* **2004**, *39*, 1033–1046. [CrossRef]
7. Stella, V.; He, Q. Cyclodextrins. *Toxicol. Pathol.* **2008**, *36*, 30–42. [CrossRef] [PubMed]
8. Raut, S.Y.; Manne, A.S.N.; Kalthur, G.; Jain, S.; Mutalik, S. Cyclodextrins as carriers in targeted delivery of therapeutic agents: Focused review on traditional and inimitable applications. *Curr. Pharm. Des.* **2019**, *25*, 444–454. [CrossRef]
9. Szente, L.; Szejtli, J. Highly soluble cyclodextrin derivatives: Chemistry, properties, and trends in development. *Adv. drug Deliv.* **1999**, *36*, 17–28. [CrossRef] [PubMed]
10. Liu, Z.; Ye, L.; Xi, J.; Wang, J.; Feng, Z.G. Cyclodextrin polymers: Structure, synthesis, and use as drug carriers. *Prog. Polym. Sci.* **2021**, *118*, 101408. [CrossRef]
11. Barman, S.; Barman, B.K.; Roy, M.N. Preparation, characterization and binding behaviors of host-guest inclusion complexes of metoclopramide hydrochloride with α- and β-cyclodextrin molecules. *J. Mol. Struct.* **2018**, *1155*, 503–512. [CrossRef]
12. Le-Deygen, I.M.; Skuredina, A.A.; Kudryashova, E.V. Drug delivery systems for fluoroquinolones: New prospects in tuberculosis treatment. *Russ. J. Bioorganic Chem.* **2017**, *43*, 487–501. [CrossRef]
13. Biwer, A.; Antranikian, G.; Heinzle, E. Enzymatic production of cyclodextrins. *Appl. Microbiol. Biotechnol.* **2002**, *59*, 609–617. [CrossRef]
14. Skuredina, A.; Le-Deygen, I.; Belogurova, N. Effect of cross-linking on the inclusion complex formation of derivatized β-cyclodextrins with small-molecule drug moxifloxacin. *Carbohydr. Res.* **2020**, *498*, 108183. [CrossRef]
15. Deygen, I.M.; Kudryashova, E.V. New versatile approach for analysis of PEG content in conjugates and complexes with biomacromolecules based on FTIR spectroscopy. *Colloids Surf. B Biointerfaces* **2016**, *141*, 36–43. [CrossRef]
16. Skuredina, A.A.; Yu Kopnova, T.; Tychinina, A.S.; Golyshev, S.A. The new strategy for studying drug-delivery systems with prolonged release: Seven-day in vitro antibacterial action. *Molecules* **2022**, *27*, 8026. [CrossRef] [PubMed]
17. Trotta, F.; Caldera, F.; Cavalli, R.; Soster, M. Molecularly imprinted cyclodextrin nanosponges for the controlled delivery of L-DOPA: Perspectives for the treatment of Parkinson's disease. *Expert Opin. Drug Deliv.* **2016**, *13*, 1671–1680. [CrossRef]
18. Skuredina, A.; Tychinina, A.; Le-Deygen, I. Cyclodextrins and their polymers affect the lipid membrane permeability and increase levofloxacin's antibacterial activity in vitro. *Polymers* **2022**, *14*, 4476. [CrossRef] [PubMed]
19. Filipe, V.; Hawe, A.; Jiskoot, W. Critical evaluation of nanoparticle tracking analysis (NTA) by NanoSight for the measurement of nanoparticles and protein aggregates. *Pharm. Res.* **2010**, *27*, 796–810. [CrossRef]
20. Takeuchi, Y.; Sunagawa, M. Stability of a 1β-methylcarbapenem antibiotic, meropenem (SM-7338) in aqueous solution. *Chem. Pharm. Bull.* **1995**, *43*, 689–692. [CrossRef]
21. Yang, S.K.; Yusoff, K.; Mai, C.W.; Lim, W.M.; Yap, W.S.; Lim, S.H.; Lai, K.S. Additivity vs. synergism: Investigation of the additive interaction of cinnamon bark oil and meropenem in combinatory therapy. *Molecules* **2017**, *22*, 1733. [CrossRef] [PubMed]
22. Skuredina, A.A.; Tychinina, A.S.; Le-Deygen, I.M.; Golyshev, S.A.; Belogurova, N.G.; Kudryashova, E.V. The formation of quasi-regular polymeric network of cross-linked sulfobutyl ether derivative of β-cyclodextrin synthesized with moxifloxacin as a template. *React. Funct. Polym.* **2021**, *159*, 104811. [CrossRef]
23. Aleem, O.; Kuchekar, B.; Pore, Y.; Late, S. Effect of β-cyclodextrin and hydroxypropyl β-cyclodextrin complexation on physicochemical properties and antimicrobial activity of cefdinir. *J. Pharm. Biomed. Anal.* **2008**, *47*, 535–540. [CrossRef] [PubMed]
24. Zhao, D.; Zhao, L.; Zhu, C.S.; Huang, W.Q.; Hu, J.L. Water-insoluble β-cyclodextrin polymer crosslinked by citric acid: Synthesis and adsorption properties toward phenol and methylene blue. *J. Incl. Phenom. Macrocycl. Chem.* **2009**, *63*, 195–201. [CrossRef]
25. Wilpiszewska, K.; Antosik, A.K.; Zdanowicz, M. The effect of citric acid on physicochemical properties of hydrophilic carboxymethyl starch-based films. *J. Polym. Environ.* **2019**, *27*, 1379–1387. [CrossRef]
26. Yilgor, I.; Yilgor, E.; Guler, I.G.; Ward, T.C.; Wilkes, G.L. FTIR investigation of the influence of diisocyanate symmetry on the morphology development in model segmented polyurethanes. *Polymer* **2006**, *47*, 4105–4114. [CrossRef]
27. Baier, G.; Baumann, D.; Siebert, J.M.; Musyanovych, A.; Mailänder, V.; Landfester, K. Suppressing unspecific cell uptake for targeted delivery using hydroxyethyl starch nanocapsules. *Biomacromolecules* **2012**, *13*, 2704–2715. [CrossRef] [PubMed]
28. Stewart, J. Vibrational spectra of primary and secondary aliphatic amines. *J. Chem. Phys.* **1959**, *30*, 1259–1265. [CrossRef]
29. Cielecka-Piontek, J.; Paczkowska, M.; Lewandowska, K.; Barszcz, B.; Zalewski, P.; Garbacki, P. Solid-state stability study of meropenem - solutions based on spectrophotometric analysis. *Chem. Cent. J.* **2013**, *7*, 2–9. [CrossRef]
30. Berthoin, K.; Le, D.C.; Marchand-Brynaert, J. Transparency declarations. *J. Antimicrob. Chemother.* **2009**, *64*, 142–150.
31. Muneer, S.; Wang, T.; Rintoul, L.; Ayoko, G.; Islam, N. Development and characterization of meropenem dry powder inhaler formulation for pulmonary drug delivery. *Int. J. Pharm.* **2020**, *587*, 119684. [CrossRef]
32. Wei, Y.; Zhang, X.; Dang, L.; Wei, H. Solubility and pseudopolymorphic transitions in mixed solvent: Meropenem in methanol–water solution. *Fluid Phase Equilib.* **2013**, *349*, 25–30. [CrossRef]
33. Kohut, A.; Demchuk, Z.; Kingsley, K.; Voronov, S.; Voronov, A. Dual role of methyl-β-cyclodextrin in the emulsion polymerization of highly hydrophobic plant oil-based monomers with various unsaturations. *Eur. Polym. J.* **2018**, *108*, 322–328. [CrossRef]
34. Sala, A.; Hoossen, Z.; Bacchi, A. Two crystal forms of a hydrated 2: 1 β-cyclodextrin fluconazole complex: Single crystal X-ray structures, dehydration profiles, and conditions for their individual. *Molecules* **2021**, *26*, 4427. [CrossRef]
35. Xu, Q.; Tang, Y.; Zhang, X.; Oshima, Y.; Chen, Q.; Jiang, D. Template Conversion of Covalent Organic Frameworks into 2D Conducting Nanocarbons for Catalyzing Oxygen Reduction Reaction. *Adv. Mater.* **2018**, *30*, 1706330. [CrossRef]

36. Mendez, A.; Chagastelles, P.; Palma, E.; Nardi, N. Thermal and alkaline stability of meropenem: Degradation products and cytotoxicity. *Int. J. Pharm.* **2008**, *350*, 95–102. [CrossRef]
37. Tomasello, C.; Leggieri, A.; Cavalli, R.; Di Perri, G.; D'avolio, A. In vitro stability evaluation of different pharmaceutical products containing meropenem. *Hosp. Pharm.* **2015**, *50*, 296–303. [CrossRef] [PubMed]